

Synthesis of Propylene Oxide from Propylene, Oxygen, and Hydrogen Catalyzed by Palladium–Platinum–Containing Titanium Silicalite

R. Meiers,* U. Dingerdissen,† and W. F. Hölderich*,¹

* Department of Chemical Technology and Heterogeneous Catalysis, University of Technology RWTH Aachen, 52074 Aachen, Germany; and † Hoechst AG, Corporate Research and Technology, 65926 Frankfurt, Germany

Received November 5, 1997; revised February 3, 1998; accepted February 3, 1998

Pt promoted and unpromoted Pd/TS-1 catalysts were prepared by impregnation with $[\text{Pd}(\text{NH}_3)_4](\text{NO}_3)_2$ and $[\text{Pt}(\text{NH}_3)_4]\text{Cl}_2$, characterized by TPR, TEM, and ESCA and tested as catalysts for the synthesis of propylene oxide (PO) from propylene, oxygen, and hydrogen. The effect of various reduction methods and Pt loading on the catalytic performance and physical characteristics of the catalysts have been studied. The autoreduction by the amine ligands under a flow of N_2 at 150°C leads to maximum PO selectivities and yields, whereas catalysts that were hydrogen reduced or calcined prior to reduction were less effective. Results obtained by ESCA and TEM show that PO formation was favoured by small Pd clusters and a high fraction of Pd(II) species. Pd agglomeration was detected on the outer surface of TS-1 crystals and was especially pronounced for calcined and reduced catalysts with cluster sizes up to 70 nm. Maximum PO yield (11.7%) with a selectivity of 46% were obtained over a TS-1 catalysts loaded with 1 wt% Pd and 0.02 wt% Pt and autoreduced under N_2 at 150°C . The increase in PO yield by adding minor amounts of Pt to a Pd/TS-1 catalyst correlates with a sharp increase in the fraction of Pd(II) species. Further addition of Pt changed the form and size of Pd clusters without further increasing the fraction of Pd(II) species, thus leading to decreasing PO yields and selectivities. © 1998 Academic Press

1. INTRODUCTION

The oxidation of propylene to propylene oxide (PO) is one of the most challenging subjects in catalysts. The invention of titanium silicate-1 (TS-1) by Taramasso *et al.* opened a new route for the synthesis of propylene oxide (1, 2). TS-1 catalyzes the epoxidation of propylene with hydrogen peroxide at high conversion rates and selectivities under mild conditions in the liquid phase. The reaction is typically carried out at $40\text{--}60^\circ\text{C}$ with methanol as the solvent (2). Because of the relatively high cost of hydrogen peroxide this process has not been commercialized up to date. In order to overcome the economic obstacle the use of hydrogen peroxide generated *in situ* is currently under research. Two different approaches are employed for the

formation of *in situ* hydrogen peroxide. The first approach makes use of the conventional anthraquinone (AQ) process for the production of hydrogen peroxide by feeding propylene and oxygen to the oxidation stage of anthrahydroquinone (AHQ). Contacting AHQ with oxygen leads to the formation of hydrogen peroxide, which is then consumed in the oxidation of propylene to PO catalyzed by TS-1 (3). The second concept is based on the oxidation of propylene by a $\text{H}_2\text{--O}_2$ gas mixture over a precious metal containing titanium silicalite. Such catalytic systems have also been tested for the oxidation of alkanes for the hydroxylation of benzene to phenol and for the oxidation of phenol (3, 4). Hydrogen peroxide is directly synthesized from H_2 and O_2 at the precious metal sites of the bifunctional catalyst and consumed as an oxidant at the Ti-sites.

For the epoxidation of propylene with a $\text{H}_2\text{--O}_2$ mixture Sato *et al.* (5–7) and Mueller *et al.* (8) employ a palladium impregnated TS-1 catalyst suspended in solvents such as water or methanol while Haruta *et al.* (9) uses a highly dispersed Au/TiO₂ catalyst in a gas phase reaction. However, the reported conversions for the oxidation of propylene with a $\text{H}_2\text{--O}_2$ mixture are below 2% and the selectivity suffers from the hydrogenation of propylene to propane. Since the generation of hydrogen peroxide seems to be the rate-determining step, we investigated opportunities to increase the PO yield by varying the precious metal species on a TS-1 catalyst. Palladium or a mixture of palladium and platinum functioned as catalysts for the *in situ* formation of hydrogen peroxide. According to Grosser *et al.* platinum enhances the rate of H_2O_2 formation (10).

The objective of the present study is to clarify the influence of the reduction methods and of the addition of platinum on the catalytic performance. Catalytic test are accompanied by TPR-, ESCA-, and TEM-analysis.

2. EXPERIMENTAL

2.1. TS-1 Synthesis

TS-1 was prepared according to the procedure described in the original TS-1 patent by Taramasso *et al.* (1); 499 g

¹ Author to whom correspondence may be addressed.

of tetraethylorthosilicate were stirred under a CO₂-free atmosphere and 15 g of tetraethyltitanate were added followed by dropwise addition of 800 g of a 25 wt% solution of tetrapropylammonium hydroxide. After the alcohol had been distilled off under vacuum at 50°C, 868 g of distilled water were added to the solution. The mixture was transferred to an autoclave, heated at 175°C and stirred under autogenous pressure for 10 days. After cooling down to room temperature, the crystalline product was separated from the liquid by centrifugation, washed with water, dried for 12 h at 120°C, and finally calcined for 10 h at 550°C in air.

2.2. Impregnation

A [Pd(NH₃)₄](NO₃)₂ solution was prepared by dissolving 10 g of Pd(NO₃)₂ in 400 g of an aqueous 25 wt% ammonia solution. After the mixture had been stirred at 50°C for 3 d, the solution was filtered and the resulting concentration of Pd was determined by ICP-analysis (21.6 mg/ml). The platinum precursor, an aqueous solution of 5.138 wt% [Pt(NH₃)₄]Cl₂, was kindly provided by Degussa AG.

Pd is supported on TS-1 by suspending 5 g of TS-1 in 20 g of deionized water and adding 2.34 ml of the [Pd(NH₃)₄](NO₃)₂ solution. The mixture was stirred at 80°C for 1 day. The solid is recovered by evaporating the solvent under vacuum at 50°C and dried at 60°C for 1 day. A catalyst containing Pd and Pt is prepared in the same way by adding 2.34 g of [Pd(NH₃)₄](NO₃)₂ solution and [Pt(NH₃)₄]Cl₂ solution to the suspended TS-1 catalyst. As determined by ICP analysis the resulting catalysts were loaded with 1 wt% Pd (cat. I1), 1 wt% Pd + 0.01 wt% Pt (cat. I2), 1 wt% Pd + 0.02 wt% Pt (cat. I3), or 1 wt% Pd + 0.1 wt% Pt (cat. I4), respectively. For reasons of simplicity we denote these impregnated TS-1 catalysts as I1 to I4.

2.3. Calcination and Reduction

The impregnated TS-1 catalyst I4 (1 wt% Pd and 0.1 wt% Pt) was subjected to different methods of calcination and reduction. Calcination was carried out according to a procedure described by Sachtler *et al.* (11) for highly dispersed Pd on ZSM-5. The catalysts were calcined in O₂ flow at 500°C for 2 h after ramping at 0.5 K/min from room temperature. They were subsequently purged with N₂ at 500°C for 20 min before cooling down to room temperature.

A second calcination procedure was conducted analogously by using air instead of O₂ as the calcination medium. The calcined samples and a merely impregnated sample were reduced with H₂ at a heating rate of 1 K/min from room temperature to 250°C. The samples were kept at 250°C for 1 h, cooled down to room temperature and purged with N₂ for 30 min.

Catalyst samples I4 were also reduced without prior calcination. Reduction was carried out with H₂, 5 vol% H₂ +

95 vol% N₂, and N₂ at a heating rate of 1 K/min from room temperature to 50, 100, 150, 200, 250, 300, or 350°C, respectively. Under pure nitrogen atmosphere the catalyst was autoreduced by thermal decomposition of the NH₃ ligands.

2.4. Propylene Epoxidation by Hydrogen and Oxygen

Since the concentration of the reactants propylene, hydrogen, and oxygen were within the explosion limits of the mixture, special safety precautions were required. We placed the reaction vessel and peripheral equipment in a barricaded area and used a remote control system to take samples, start, monitor, and terminate the reaction. All runs were conducted as batch experiments. The reactor consisted of a 200 ml stainless steel autoclave equipped with two inlets for propylene and gaseous reactants, an outlet, a temperature indicator, and a pressure indicator. An outer jacket was provided through which water at a constant temperature could be circulated. Liquid propylene was pumped into the autoclave while H₂, O₂, and N₂ were supplied through mass flow controllers. The reaction mixture was stirred by a stirring bar that was placed inside the reactor and driven by a magnetic stirrer.

In a typical run 15 g of methanol, 5 g of deionized water, and 0.2 g of catalyst are charged to the autoclave. Air was removed by purging with N₂. After 10 g of propylene were fed into the reactor the vessel was pressurized with hydrogen (7 bar), nitrogen (15 bar), and oxygen (10 bar) in succession. The slurry was heated from room temperature to 43°C under pressure and vigorous stirring. The reactor was kept for 2 h at 43°C and then cooled down to 15°C. Since all runs were batch experiments a pressure drop during the reaction was observed.

At the end of the reaction the entire gas phase was discharged into a gas bag (Linde Plastigas[®]). The catalyst was filtered off the liquid phase and *t*-butyl methyl ether (MTBE) was added as the external standard. Ethylene was added to the gas phase as a reference substance via a gas meter. Liquid phase analysis was performed on a Carlo Erba Z 2300 gas chromatograph, using a flame ionization detector and a 4-m column Carborwax 1500 as the stationary phase. For the gas phase analysis a 3-m Porapack 1500 column was used in connection with a thermal conductivity meter.

In order to check the catalytic performance of the nonimpregnated TS-1 a test reaction was carried out by epoxidizing propylene with H₂O₂ over TS-1. The conditions applied were as stated above, except that 8 g of aqueous 30 wt% H₂O₂ was used, instead of the H₂-O₂ mixture.

We used the PO-yield and PO-selectivity to describe the results of the catalytic experiments. Since the resulting conversion can be calculated from the yield and selectivity, the conversion is not presented in most tables and figures. PO yield is based on propylene and PO selectivity is based on all organic products.

2.5. Catalyst Characterization

X-ray powder diffraction analysis (XRD) were performed on a Siemens D 5000 diffractometer equipped with CuK_α radiation. Diffuse reflectance UV-Vis (DR-UV-Vis) spectra were obtained with a Lambda 7 spectrometer from Perkin Elmer. Diffuse reflectance IR (DRIFT) was carried out by means of a Praying-Mantis-Unit from Harric. The chemical composition of the catalysts were determined by an ICP spectroflame D.

For temperature-programmed reduction (TPR) samples were reduced with 5 vol% H_2/Ar as described elsewhere (12). The temperature was ramped with 6 K/min from room temperature to 600°C.

ESCA spectra of reduced Pd/TS-1 and Pd-Pt/TS-1 samples were recorded on a PHI 5600 using AlK_α radiation at a power of 300 W. The pressure in the spectrometer during measurement was 2×10^{-8} Torr (1 Torr = 133.3 Nm⁻²). An overview spectra was recorded at a pass energy of 117.4 eV while a more detailed spectra was recorded at a pass energy of 29.4 eV.

Pd/TS-1 and Pd-Pt/TS-1 samples in the reduced from were examined by transmission electron microscopy (TEM). The powders were dispersed on a holey carbon coated copper grid. The sample 1 wt% Pd/TS-1 was analyzed by a Phillips CM 30 microscope with an acceleration voltage of 300 kV. Any other micrographs were taken using a JEOL JEM-2000 FX II at an acceleration voltage of 200 kV.

3. RESULTS AND DISCUSSION

3.1. TS-1 Characterization

Elemental analysis of TS-1 by ICP gave a molar ratio of Si/Ti = 34.6. Crystalite sizes are in the range of 0.1–0.3 μm . X-ray diffractometry confirmed the MFI-structure of the synthesized TS-1 samples. The DRIFT spectra reveals a

band at 960 cm⁻¹ which is in agreement with literature data (13). The DR-UV-Vis spectrum presents of band in the range of 190–210 nm, indicating tetrahedrally coordinated titanium atoms (13).

We evaluated the capability of TS-1 for the epoxidation of propylene with H_2O_2 . The results of the epoxidation reaction after 3 h under the conditions stated above were: H_2O_2 conversion, 100%; PO yield, 40% (based on H_2O_2); selectivity, 94% (based on all organic products).

3.2. Effect of Reduction Method

3.2.1. Calcined and reduced Pd-Pt/TS-1. In Table 1 the catalytic performance of catalyst samples I4 that were calcined (air/ O_2 , 500°C) prior to reduction is compared to an uncalcined I4 catalyst that was reduced under the same conditions (H_2 , 250°C). The propylene conversion of 8% was lowest for the uncalcined catalyst. Calcination under O_2 leads to an increase of the conversion to 32% while the conversion increases to 44% by calcination under air. The selectivities obtained by the calcined and uncalcined catalysts were below 2%, thereby leading to insignificant PO-yields. The main by-product formed was propane with selectivities above 97% for all three catalysts. Further by-products formed were 1-Methoxy-2-propanol, 1,2-propanediol, and 2-methoxy-1-propanol with a combined selectivity of less than 2%. Calcination of the I4 catalyst therefore increases the propane formation as demonstrated by the increase of the conversion.

Variations of the calcination and the reduction methods did not cause any significant change in the selectivity and PO-yield as shown in Table 1. For this reason we stopped using any calcination prior to reduction and investigated the effect of different reduction methods on the catalytic performance of catalyst I4.

3.2.2. Influence of reduction method on catalytic performance. The effect of different reduction methods on the

TABLE 1

Epoxidation of Propylene with H_2 and O_2 over Calcined and Reduced TS-1 Catalyst Loaded with 1 wt% Pd and 0.1 wt% Pt

Calcination			Reduction			Catalytic performance		
Medium	T [°C]	t [h]	Medium	T [°C]	t [h]	Propylene conversion [%]	PO selectivity [%]	PO yield [%]
—	—	—	H_2	250	3	8.3	2.1	0.2
O_2	500	2	H_2	250	3	31.7	0.9	0.3
Air	500	2	H_2	250	3	44.1	1.1	0.5
Air	500	12	H_2	250	1	26.1	6.6	1.7
Air	450	2	H_2	250	1	30.6	1.8	0.6
Air	500	12	H_2	50	14	31.6	5.1	1.6
Air	250	2	5% H_2/N_2	50	1	59.5	1.4	0.9
Air	200	2	5% H_2/N_2	50	1	53.3	3.7	2.0

Note. Conditions: 0.2 g catalyst, 15 g MeOH, 5 g H_2O , 10 g propylene, 7 bar H_2 (59 mmol), 15 bar N_2 (138 mmol), 10 bar O_2 (92 mmol), 2 h, 43°C.

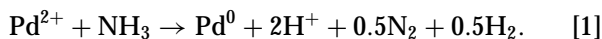
TABLE 2

PO Yield over Differently Reduced 1 wt% Pd + 0.1 wt% Pt/TS-1 Catalysts

Reduction temperature [°C]	Reduction medium		
	H ₂	5% H ₂ + 95% N ₂	N ₂
50	2.3	2.2	2.7
100	0	0.4	2.5
150	0	3.5	5.3
200	1.1	4.1	3.3
250	0.2	2	3.5
300	1.4	2.5	1.8
350	1.1	2.7	2.1

Note. Conditions: 0.2 g catalyst, 15 g MeOH, 5 g H₂O, 10 g propylene, 7 bar H₂ (59 mmol), 15 bar N₂ (138 mmol), 10 bar O₂ (92 mmol), 2 h, 43°C.

catalytic performance was studied by reducing catalyst I4 under an atmosphere of H₂, 5% H₂/N₂, or N₂ at temperatures ranging from 50 to 350°C. The resulting PO yields and selectivities are displayed in Tables 2 and 3. Two trends, one related to the gaseous medium used and one related to the temperature, can be observed. PO yield and PO selectivity are favoured by reduction under a pure nitrogen atmosphere. These catalysts are autoreduced as the thermal decomposition of the amine complex creates locally a reducing atmosphere (14, 15):



Increasing the hydrogen concentration in the reduction medium causes the PO-yield and selectivity to decrease. The catalyst reduced with pure hydrogen gave the lowest yield and selectivity. The effect of the reduction temperature was most significant for the catalyst reduced under nitrogen. These autoreduced samples exhibited a peak in the PO yield of 5.3% at a reduction temperature of 150°C. When 5% H₂/N₂ was employed the maximum PO yield

TABLE 3

PO Selectivity over Differently Reduced 1 wt% Pd + 0.1 wt% Pt/TS-1 Catalysts

Reduction temperature [°C]	Reduction medium		
	H ₂	5% H ₂ + 95% N ₂	N ₂
50		4.9	5.2
100		3.2	4.2
150		12.3	11.1
200	7.2	14.3	10.1
250	3.1	6.2	18.8
300	3.6	7.8	4.5
350		16.2	3.4

Note. Conditions: 0.2 g catalyst, 15 g MeOH, 5 g H₂O, 10 g propylene, 7 bar H₂ (59 mmol), 15 bar N₂ (138 mmol), 10 bar O₂ (92 mmol), 2 h, 43°C.

of 4.1% was in the range of 150–200°C. Because of the very low PO yields of the hydrogen-reduced catalyst no clear trend can be observed with those catalysts. Selectivities of all tested catalysts were below 20%. As in the case of the calcined catalysts propane is the main by-product. Further by-products formed were 1-Methoxy-2-propanol, 1,2-propane diol, and 2-methoxy-1-propanol with a combined selectivity of less than 5%.

Interestingly, PO was even formed over a catalyst (50°C, N₂) not reduced prior to catalytic testing. This catalyst was used in the impregnated form without any further treatment and achieved a PO yield of 2.7% at a selectivity of 5.2%. During the reaction this catalyst changed its colour from white to grey which can be taken as evidence for the fact that the catalysts undergo reduction during the reaction. Such catalysts reduced under reaction conditions performed better than or equal to those catalysts reduced with pure hydrogen or at temperatures above 300°C (Table 2).

3.3. Influence of Platinum Loading on Catalytic Performance

It can be concluded from the results obtained that the PO formation is favoured by “mild” reduction conditions, i.e. no calcination step prior to reduction, reduction temperatures below 200°C, and a very low hydrogen concentration in the catalyst bed during reduction. Although we were able to improve the PO yield by varying the reduction methods we could not suppress the propane formation sufficiently. The platinum loading of 0.1% offered an explanation for the low PO selectivities as platinum is known for its hydrogenation activity. In order to verify this assumption we conducted a series of experiments over catalysts with 1% palladium and varying platinum loadings: 0%, 0.01%, 0.02%, 0.1% (catalysts I1 to I4). The impregnated catalysts were autoreduced under nitrogen atmosphere at 150°C. For reasons of simplicity we denote the autoreduced catalysts as catalyst A1 (1 wt% Pd/TS-1), catalyst A2 (1 wt% Pd + 0.01 wt% Pt), catalyst A3 (1% Pd + 0.02% Pt), and catalyst A4 (1% Pd + 0.1% Pt).

Figure 1 presents the PO yield and PO selectivity as a function of platinum loading. Over the platinum-free catalyst A1 a PO yield of 8.2% was achieved with a selectivity of 23.4%. By adding as little as 0.01 or 0.02 wt% Pt to the 1 wt% Pd/TS-1 catalyst the yield increased to 10.3 or 11.7%, respectively. The increase in yield was accompanied by an increase in the selectivity: 41.0% over catalyst A2 and 46.0% over catalyst A3. A platinum loading of 0.1 wt% (catalyst A4) led to a decrease in yield and selectivity: PO yield = 5.3%, selectivity = 11.1%.

These results demonstrated that the platinum loading is a highly sensitive parameter that should not exceed 0.02 wt% to achieve maximum PO yields and PO selectivities. The improvement in PO yield by adding platinum to a Pd catalyst is in accordance with results reported by Grosser *et al.*, who

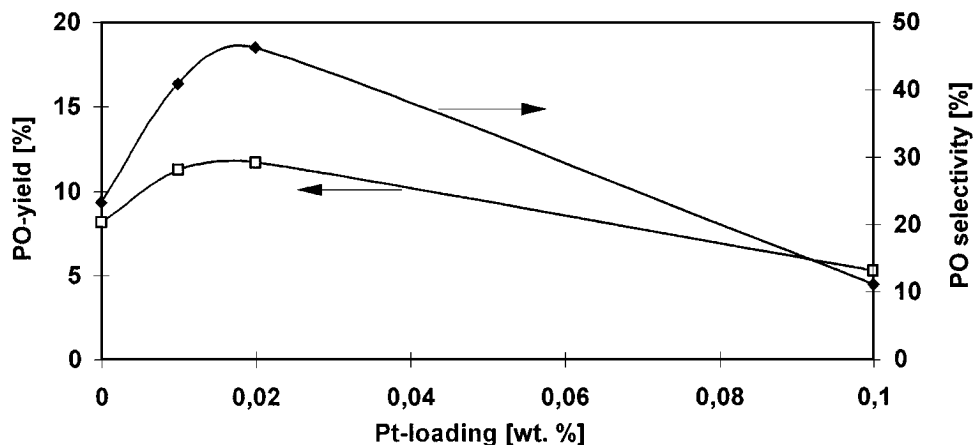


FIG. 1. Epoxidation of propylene with H_2 and O_2 over 1 wt% Pd + x wt% Pt/TS-1. Reduction: 150°C, N_2 . Conditions: 0.2 g catalyst, 15 g MeOH, 5 g H_2O , 10 g propylene, 7 bar H_2 (59 mmol), 15 bar N_2 (138 mmol), 10 bar O_2 (92 mmol), 2 h, 43°C.

found that platinum-promoted Pd catalysts were superior in the direct synthesis of H_2O_2 , compared to platinum-free catalysts. Although the selectivity improved significantly by adding only minor amounts of platinum to the Pd/TS-1 catalyst, the formation of propane was still dominant.

3.4. Characterization of Pd and Pt Species

3.4.1. Characterization by TPR. In order to figure out at what temperatures Pd and Pt were reduced on an impregnated TS-1 catalysts we performed TPR analysis. The TPR spectrum of a 1% Pd/TS-1 and a 1% Pd + 1% Pt/TS-1 catalyst are shown in Fig. 2. The spectrum of the 1% Pd/TS-1 catalyst exhibits two reduction peaks centered around 150°C that were too close to be resolved. The reduction commenced at ca 60°C and was completed at ca 250°C. Two reduction peaks were observed for TS-1 impregnated with $[Pd(NH_3)_4](NO_3)_2$ and $[Pt(NH_3)_4]Cl_2$. In addition to the palladium reduction peak centered around 160°C, a sec-

ond peak centered around 110°C appeared, which can be assigned to the reduction of platinum. The TPR data fits well into the catalytic data on the effect of reduction methods (Tables 2 and 3) as maximum PO yields were achieved with reduction temperatures of 150°C. In order to find out at which temperatures the amine ligands decompose in the absence of hydrogen, we studied the thermal reaction of a 1% Pd + 1% Pt/TS-1 catalyst under the flow of pure helium instead of H_2/Ar , using otherwise the same conditions as for the TPR experiments. We observed a peak centered around 230°C. Hence the presence of hydrogen seems to lower the temperature at which the decomposition of the amine ligands and thus the reduction of the precious metall takes place.

To evaluate the effect of calcination on Pd reduction we subjected to TPR analysis a TS-1 catalyst that was impregnated with 1 wt% Pd and 0.1 wt% Pt and calcined under air at 500°C for 5 h. In this case palladium was immediately reduced at the beginning of the TPR at room temperature which is in accordance with results obtained for calcined Pd containing zeolites (12). This result explains also why the catalysts calcined under air could be reduced with 5 vol% H_2/O_2 at 50°C (Table 1).

3.4.2. Characterization by TEM. Results obtained by transmission electron microscopy (TEM) are summarized in Table 4. Two new parameters describing the form of Pd clusters and the homogeneity of Pd dispersion on the crystal surface are introduced in addition to minimum and maximum cluster size. The shape of the Pd clusters was either circular (●) or needle-like (—). Dispersion of Pd clusters ranged from "very homogeneous" (++) to "very inhomogeneous" (—).

A result in common for all examined samples was the minimum cluster size that was in the range of 2–3 nm (Fig. 3). Since the pore size of TS-1 is 0.55–0.56 nm it is unlikely that Pd clusters exist within the pore system of the

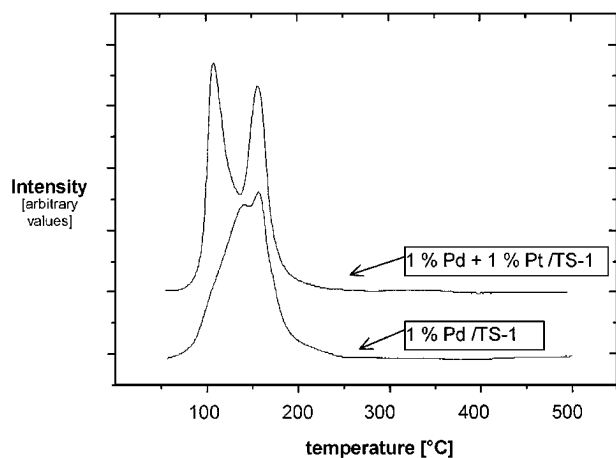


FIG. 2. TPR spectrum of sample 1 wt% Pd/TS-1 and 1 wt% Pd + 1 wt% Pt/TS-1.

TABLE 4
Size, Form, and Homogeneity of Pd Clusters

Pd wt%	Pt wt%	Reduction method	Homogeneity of cluster distribution	Cluster form	Cluster size [nm]	
					Max.	Min.
1	0	150°C-N ₂	+	—	30	5
1	0.01	150°C-N ₂	+	●	15	2
1	0.02	150°C-N ₂	○	●	40	5
1	0.1	150°C-N ₂	—	●	25	3
1	0.1	150°C-5% H ₂	—	●	20	2
1	0.1	150°C-H ₂	—	●	15	2
1	0.1	200°C-5% H ₂	++	●	14	3
1	0.1	200°C-H ₂	++	●	20	3
1	0.1	500°C-air 250°C-H ₂	---	●	70	2

TS-1 crystals. This constitutes a major difference to Pd ion exchanged zeolites like H-ZSM-5, where Pd can be found inside the zeolite pores (11).

Figure 4 represents a TEM micrograph of sample I4 (1 wt% Pd + 0.1 wt% Pt/TS-1) that was calcined under air at 500°C and reduced with H₂ at 250°C. In contrast to the uncalcined samples we found extremely large clusters in the range of 50–70 nm that were formed by palladium agglomeration as confirmed by EDX analysis. These large agglomerations were distributed very inhomogeneously and were found only on few TS-1 crystals. Apart from the large Pd agglomeration small Pd clusters with a particle size of 2–5 nm were distributed homogeneously over the zeolite surface. Clusters with particle sizes between these two extremes were very rare and were only present among the large Pd agglomerations.

The three catalyst samples I4 (1 wt% Pd and 0.1 wt% Pt) that were reduced at 150°C with H₂, 5 vol% H₂/N₂ or N₂, did not reveal any difference in particle size or

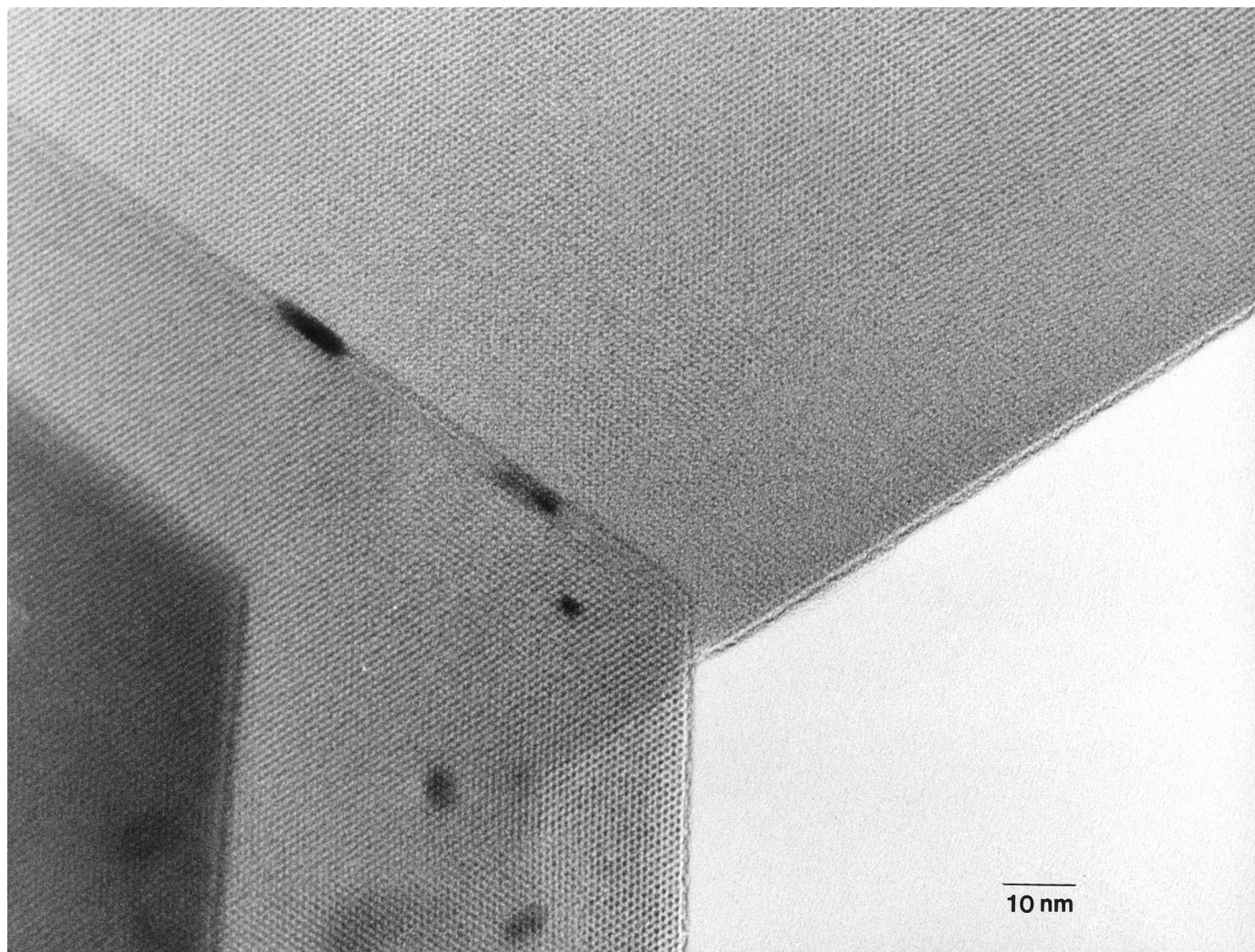


FIG. 3. TEM micrograph of 1 wt% Pd/TS-1 (reduction: 150°C, N₂).

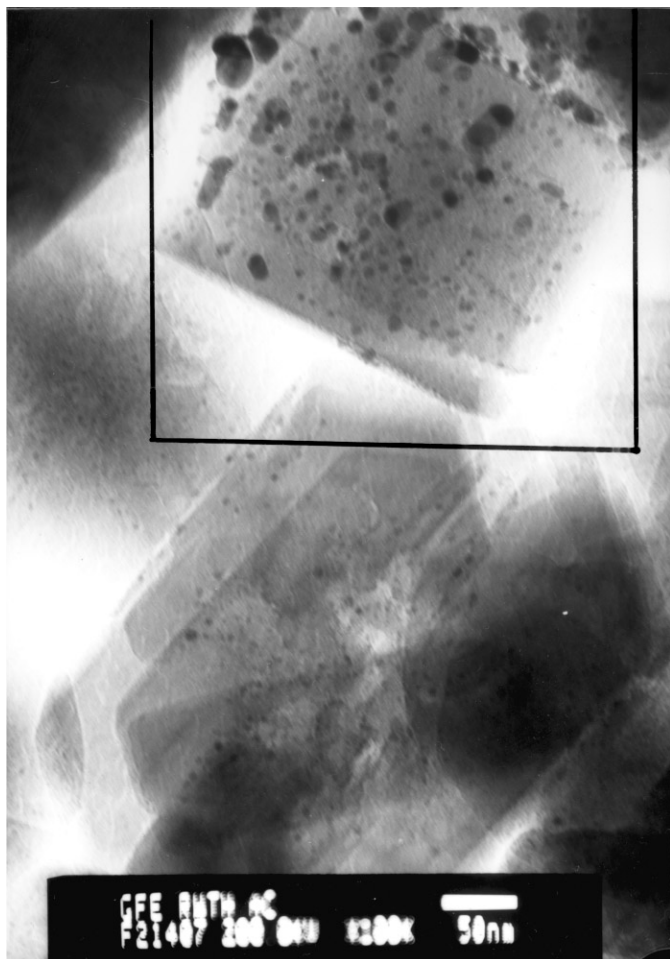


FIG. 4. TEM micrograph of 1 wt% Pd + 0.1 wt% Pt/TS-1 (calcination: 500°C under air, reduction: 250°C, H₂).

distribution (Table 4). This is a very important result, because these three catalysts do indeed exhibit significant differences in the catalytic performance (Tables 2 and 3). As the TEM data do not reveal any differences in the Pd dispersion, the catalyst activity and selectivity must be affected by another dominant factor.

Clusters sizing from 2–20 nm were distributed inhomogeneously. As an example the autoreduced sample (150°C, N₂) is shown in Fig. 5. A TEM micrograph of sample I4 that was reduced at 200°C with H₂ is shown in Fig. 6. Only few small clusters in the range of 2–4 nm were present while most clusters sizes were in the range of 7–10 nm. This was also true for the sample reduced with 5 vol% H₂/N₂ at 200°C. Therefore, it can be suggested that an increase in reduction temperatures lead to particle agglomeration, which is a well-known effect for Pd-containing catalysts (16).

The addition of platinum to Pd/TS-1 catalysts had a significant effect on the Pd clusters as the results in Table 4 demonstrate. Catalysts were autoreduced at 150°C under N₂ and Pd loading was 1% while Pt loading varied from

0–0.1 wt%. Figure 7 shows the micrograph of the platinum-free sample. Apart from the common circular clusters we find needle-shaped clusters as long as 40 nm. The particles were distributed homogeneously over the zeolite surface. The size of the circular shaped clusters did not exceed 15 nm. Adding more than 0.02 wt% platinum to the catalysts caused the needle-shaped clusters to disappear. An explanation for this effect cannot be given. By increasing the platinum loading of the catalysts the homogeneity of particle distribution decreases as the results in Table 4 indicate.

The observation of large Pd clusters is in sharp contrast to Pd cluster sizes found on ion-exchanged zeolites as Pd/HZSM-5 that were calcined and reduced in the same way. According to Sachtler *et al.* the size of Pd clusters were less than 1 nm for a Pd/HZSM-5 sample after calcination (500°C, O₂) and reduction (250°C, H₂). Unlike HZSM-5 the TS-1 catalyst contains neither Al-atoms nor Brønsted sites. Therefore, transition metals cannot be anchored to an Al anions as in the case of HZSM-5 or other zeolites.

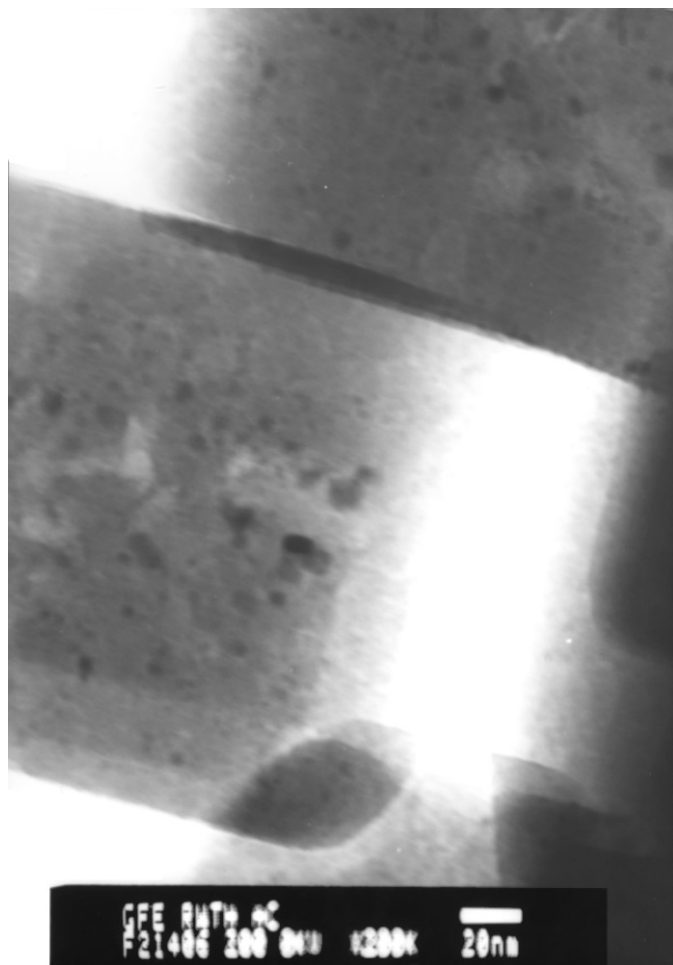


FIG. 5. TEM micrograph of 1 wt% Pd + 0.1 wt% Pt/TS-1 (reduction: 150°C, N₂).

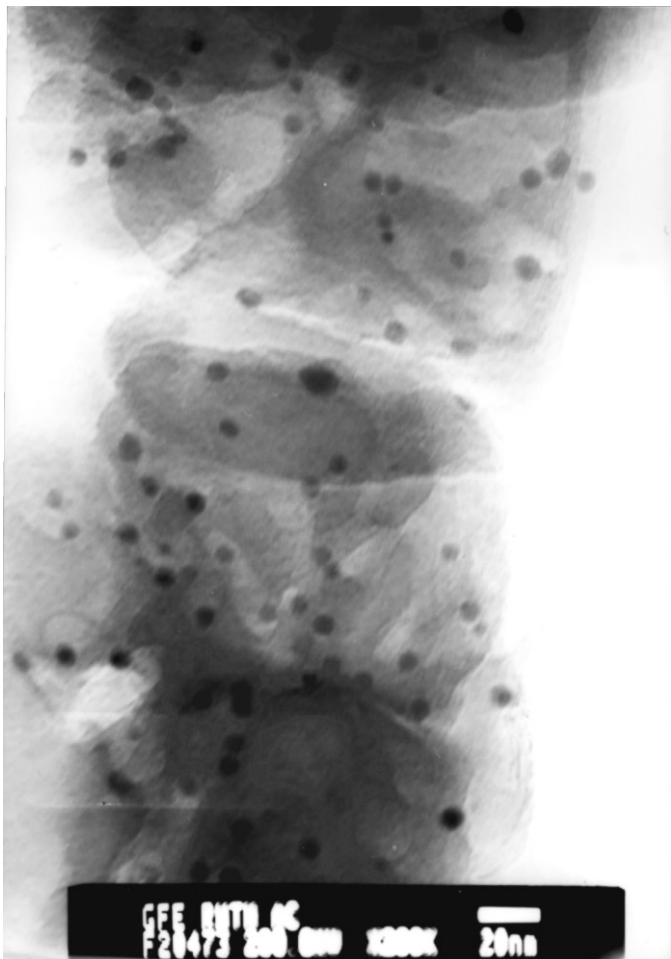
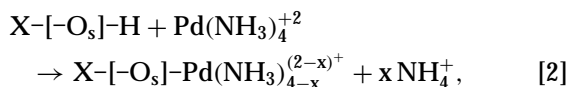


FIG. 6. TEM micrograph of 1 wt% Pd + 0.1 wt% Pt/TS-1 (reduction: 200°C, H₂).

However, due to the presence of hydroxyl groups, palladium tetraamine ions can be anchored to the surface by ion exchange according to reaction [2],



where $[-\text{O}_s]-$ stands for a surface ion (14). Since hydroxyl groups in the form of Si-OH groups are also present in TS-1, it can be assumed that part of the Pd loading is anchored to silanol groups while the rest is physically adsorbed to the TS-1 surface. As the interaction between the physically adsorbed Pd and the lattice is not as strong as the interaction between Pd and the silanol groups it is likely that the physically adsorbed Pd preferentially agglomerates to large clusters, especially when high temperatures are applied. Migration and agglomeration of Pd anchored to silanol groups is less likely. Assuming two differently adsorbed Pd species explains why the smallest cluster size found on Pd/TS-1 (2 nm) was independent of the reduction method while the

largest clusters were strongly dependent on the reduction method applied.

3.4.2. Characterization by ESCA. The ESCA study was carried out to assess the oxidation state of the Pd clusters as a function of reduction methods and platinum loading. Binding energies of the Pt-species could not be measured because the Pt signal of the platinum-containing catalysts was too weak. The results of the ESCA-study are compiled in Table 5. The binding energies for three different Pd species were found. The binding energy (BE) and Pd species were correlated according to Neumann (17) and Briggs and Seah (18). Binding energies ranging from 335.3–335.5 eV were assigned to Pd⁰, which is in good agreement with the BE of Pd^{metal} (335.0 eV). The exposure to air shifted the BE to higher values.

No species in the state of Pd⁰ were found on two samples: catalyst I4 (1 wt% Pd + 0.1 wt% Pt/TS-1) autoreduced under N₂ at 150°C and catalyst I4 reduced with 5 vol% H₂/N₂ at 150°C. Instead, values for BE were in the range of 336.1–336.2 eV which is close to the BE for PdO. Since the presence of PdO cannot be explained by a calcination step, we assume that this effect is due to a prolonged exposure of Pd⁰ species to air.

Every catalyst examined was covered by Pd species with BE ranging from 337.2–337.8 eV. The same BE value was observed for a sample impregnated with 1 wt% Pd that was not reduced prior ESCA analysis. The BE value for this Pd species cannot be easily attributed to Pd binding energies found in the literature. If one assumes that PdO₂, which shows also a peak at 337.9 eV (18), caused this signal, then the merely impregnated catalyst would be covered with PdO₂ and would show a dark red colour, which is not the case. Therefore, it can be excluded that PdO₂ is the cause of this BE. This ESCA signal cannot be caused by the Pd precursor itself, [Pd(NH₃)₄]Cl₂, because BE of Pd 3d5/2 were reported at 338.4 eV for this Pd compound. As the catalyst support influences the BE values for Pd(II) we assume that

TABLE 5
ESCA Results

Pd wt%	Pt wt%	Reduction	Pd ⁰		PdO		Pd(II)	
			eV	%	eV	%	eV	%
1	0	Not reduced					337.3	100
1	0	150°C-N ₂	335.5	88			337.7	12
1	0.01	150°C-N ₂	335.3	57			337.8	43
1	0.02	150°C-N ₂	335.4	47			337.7	53
1	0.1	150°C-N ₂			336.1	44.3	337.8	55.7
1	0.1	150°C			336.2	69.9	337.8	27.5
		5% H ₂ + 95% N ₂						
1	0.1	150°C-H ₂	335.4	72.5			337.2	27.5
1	0.1	500°C-air	335.3	81.8			337.4	18.2
		250°C-H ₂						

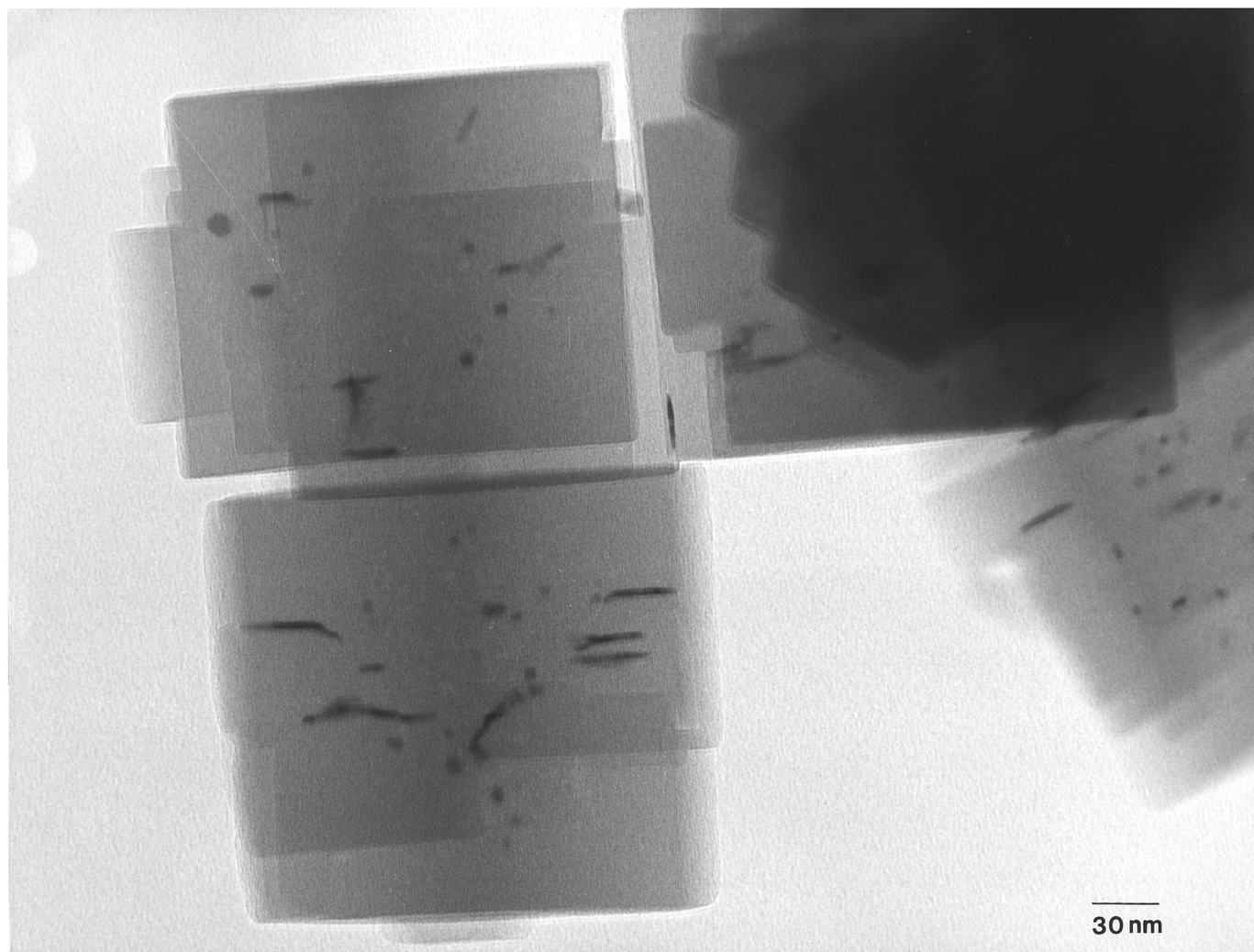


FIG. 7. TEM micrograph of 1 wt% Pd/TS-1 (reduction: 150°C, N₂).

the interaction of the Pd precursor, [Pd(NH₃)₄]Cl₂, with the TS-1 support creates a Pd species with a BE value ranging from 337.2–337.8 eV. For reasons of simplicity we denote this species as Pd(II).

In the following sections we will look for correlations between the oxidation state of Pd and the catalytic results. As the Pd(II) species was present in all catalysts we use the fraction of Pd(II) species given in percentages to describe the oxidation state of Pd and to relate it to the reduction method and the platinum loading. (It is important to keep in mind that the reduction method and the platinum loading do not only affect the oxidation state of Pd but also the Pd dispersion. Although we were able to assess the Pd dispersion by TEM, we are aware of the fact that this method provides only qualitative data.)

Table 6 demonstrates the effect of the reduction method on the PO yield, PO selectivity, and the fraction of the Pd(II) species for a catalyst I4 (1 wt% Pd + 0.1 wt% Pt/TS-1).

Three catalysts were reduced at 150°C with N₂, 5 vol% H₂/N₂, or H₂ and the fourth catalyst was first calcined under air at 500°C and subsequently reduced with H₂ at 250°C. The fraction of Pd(II) species, that was found to be the highest for the autoreduced catalyst (56%), decreased

TABLE 6
Effect of Reduction Method on Pd(II) Species, PO Yield, and PO Selectivity for a 1% Pd + 0.1% Pt/TS-1 Catalyst

Reduction method [%]	Pd(II) [%]	PO yield [%]	PO selectivity [%]
150°C–N ₂	55.7	5.8	15
150°C–5% H ₂ /N ₂	30.1	3.6	12.3
150°C–H ₂	27.5	0.2	1.6
500°C–air	18.2	1.2	3.9
350°C–H ₂			

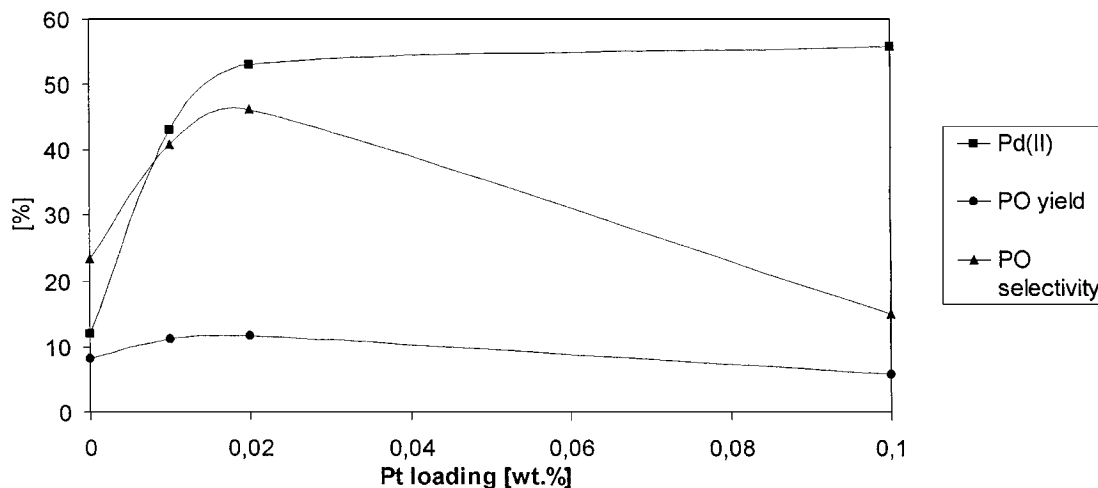


FIG. 8. Effect of platinum loading on Pd(II) species and PO yield and selectivity.

drastically to 28% for the catalyst reduced with 5 vol% H_2/N_2 or H_2 . The calcined and reduced sample contained the least amount of Pd(II) species (18%). As expected the more severe the reduction conditions were, the more Pd was reduced to Pd^0 . However, it is remarkable that the Pd species, even on the calcined and reduced sample, was not completely reduced to Pd^0 , although calcination and reduction conditions should create a fully reduced catalyst. The presence of platinum offers an explanation for this effect which is validated by the results presented in Fig. 8. The decrease of the fraction of Pd(II) species was accompanied by a sharp decrease in PO yield and a slightly decreasing PO selectivity.

As described in the previous section the I4 catalysts reduced at 150°C using different reduction mediums do not show any differences in the Pd dispersion. Therefore, the fraction of Pd(II) species constitutes the major difference between these catalysts and must thus be responsible for the catalytic performances of the catalysts. For these reasons it can be concluded that the formation of PO is favoured by the Pd(II) species.

In order to assess the influence of platinum loading on Pd reduction, we subjected the catalysts presented in Fig. 1 to ESCA analysis (see Fig. 8). These samples were impregnated with 1.0 wt% Pd and various amounts of Pt (0–0.1 wt%) and were autoreduced under nitrogen at 150°C. The fraction of Pd(II) species increased sharply from 12% for the platinum-free 1 wt% Pd/TS-1 catalyst to 43% for the catalyst containing 0.01 wt% Pt. By further increasing the Pt loading to 0.02 and 0.1 wt% the fraction of Pd(II) species increased to 53 and 56%, respectively. While the fraction of Pd(II) species is nonlinear, related to the platinum loading for 0–0.02 wt% Pt, the fraction of Pd(II) species seems to reach to a saturation level for platinum loadings higher than 0.02 wt%. The increase of Pd(II) by adding Pt to the Pd/TS-1 catalyst can be attributed to the fact that plat-

inum is more precious palladium. Therefore, Pd(II) species was found even on the calcined and reduced 1 wt% Pd + 0.1 wt% Pt/TS-1 catalyst (see Table 6).

As shown in Fig. 8 the PO yield and the PO selectivity reached a maximum at a Pt loading of 0.01–0.02 wt%. In the previous section we have stated that the formation of PO is favoured by Pd(II) species. On first sight this is in contrast to the observation that the PO yield, after reaching its maximum, did not increase in parallel with an increasing fraction of Pd(II), as shown in Fig. 8. The addition of platinum, however, did not cause only the fraction of Pd(II) species to increase but it affected also the form and distribution of Pd clusters on the crystal surface as described above. We observed that the decrease in PO yield, after reaching its maximum at 0.02 wt% Pt, coincided with the disappearance of needle-shaped Pd clusters and with less homogeneously distributed clusters. The effect of platinum on the Pd clusters seems to counteract the effect on the oxidation state of Pd. Therefore, the peak in PO yield around 0.02 wt% Pt is probably due to the pronounced increase of the fraction of Pd(II) species for Pt loadings between 0–0.2 wt% which is eclipsed by the change of Pd clusters for Pt loadings above 0.02 wt%. Apart from these two effects of platinum on the PO formation, platinum itself catalyzes the hydrogenation of propylene to propane, which caused the selectivity to decrease for Pt loadings above 0.02 wt%.

Future research must quantify the Pd dispersion more precisely in order to separate the effect of the Pd oxidation state and the Pd dispersion.

CONCLUSIONS

The physical characteristics and the catalytic performance of Pd–Pt/TS-1 catalysts depend strongly on the reduction method and the platinum loading. The formation of PO was found to be favoured by a high fraction of the

Pd(II) species and by small Pd clusters, whereas fully reduced Pd and large clusters favoured propane production. The fraction of Pd(II) was increased by autoreduction of the tetraamine ligand in the absence of hydrogen in the reduction medium. Reduction temperatures above 150°C or calcination led to cluster agglomeration on the external TS-1 surface and thus to decreasing PO yields and PO selectivities. Adding minor amounts of platinum also drastically increased the fraction of Pd(II) species in comparison to the Pd⁰ species. Since platinum effects the Pd cluster size and distribution and catalyzes also the hydrogenation of propylene to propane, there is an optimum Pt loading to achieve maximum PO yields and selectivities in the range of 0.01–0.02 wt% Pt.

ACKNOWLEDGMENTS

Financial support of the Hoechst AG is gratefully acknowledged. The authors thank Professor Kühlein and Dr. Schulz for helpful discussions and Dr. Althoff and Dr. Bestgen for providing ESCA and TEM characterizations.

REFERENCES

1. Taramasso, M., Perego, G., and Notari, B., U.S. Patent 4,410,501 to Snamprogetti S.p.A. (1983).
2. Clerici, M. G., Bellussi, G., and Romano, U., *J. Catal.* **129**, 159 (1991).
3. Ingallina, P., Clerici, M. G., Rossi, L., and Bellusi, G., *Stud. Surf. Sci. Catal.* **92**, 31 (1995).
4. Tatsumi, T., Yuasa, K., and Tominaga, H. J., *Chem. Soc., Chem. Commun.*, 1446 (1992).
5. Sato, M., and Miyake, T., Jp. Patent 4,352,771 (1992).
6. Sato, A., Oguri, M., Tokumaru, M., and Miyake, T., Jp. Patent Appl. 269,029 to Tosoh (1996).
7. Sato, A., Oguri, M., Tokumaru, M., and Miyake, T., Jp. Patent Appl. 269,030 to Tosoh (1996).
8. Müller, U., Lingelbach, P., Bassler, P., Harder, W., Karsten, E., Kohl, V., Dembowski, J., Rieber, N., and Fischer, M., German Patent Appl. DE 44 25 672 A1 to BASF AG (1996).
9. Haruta, M., and Hayashi, T., *Shokubai* **37**, 72 (1995).
10. Grosser, L. W., and Schwarz, J.-A. T., U.S. Patent 4,832,938 (1989).
11. Zhang, Z., Lerner, B., Lei, G.-D., and Sachtler, W. M. H., *J. Catal.* **140**, 481 (1993).
12. Hurst, N. W., Gentry, St. J., Jones, A., and McNicol, B. D., *Catal. Re.-Sci. Eng.* **24**, 233 (1982).
13. Bellussi, G., and Rigutto, M. S., in "Advanced Zeolite Science and Applications" (J. C. Jansen, M. Stöcker, H. G. Karge, and J. Weitkamp, Eds.), *Stud. Surf. Sci. Catal.*, Vol. 85, p. 177. Elsevier, Amsterdam/New York, 1994.
14. Albers, P., and Kiwi, J., *J. Mol. Catal.* **58**, 115 (1990).
15. Novakova, J., Kubelkova, L., Brabec, L., Bastl, Z., Jaeger, N., and Schulz-Ekloff, G., *Zeolites* **16**, 173 (1996).
16. Sachtler, W. M. H., and Zhang, Z., in "Advances in Catalysis" (D. Eley and P. Weisz, Eds.), Vol. 39, p. 129. Academic Press, New York, 1993.
17. Neumann, M., Ph.D. thesis, University of Frankfurt, 1995.
18. Briggs, D., and Seah, M. P. (Eds.), "Practical Surface Analysis, Auger and X-Ray Photoelectron Spectroscopy," 2nd ed., Vol. 1, Wiley, Chichester, 1990.